KfK 2962

KfK 2962
Dezember 1980

Current Status of Modeling Fission Gas Behaviour in the Karlsruhe Code LANGZEIT / KURZZEIT

L. Väth
Institut für Neutronenphysik und Reaktortechnik
Projekt Schneller Brüter

Kernforschungszentrum Karlsruhe

KERNFORSCHUNGSZENTRUM KARLSRUHE

Institut für Neutronenphysik und Reaktortechnik
Projekt Schneller Brüter

KfK 2962

Current Status of Modeling Fission Gas Behaviour in the Karlsruhe Code LANGZEIT/KURZZEIT

L. Väth

Kernforschungszentrum Karlsruhe GmbH, Karlsruhe

Kernforschungszentrum Karlsruhe GmbH
ISSN 0303-4003

Abstract

The programme LANGZEIT/KURZZEIT has been recently extended to describe intragranular bubble coalescence and volume equilibration, to model intergranular gas behaviour and transient release from closed porosity. The model is described and the results of some comparisons with transient experiments are discussed. Further necessary refinements of the model are outlined.

Gegenwärtiger Stand der Modellierung des Spaltgasverhaltens in dem Karlsruher Code LANGZEIT/KURZZEIT

Zusammenfassung

Das Programm LANGZEIT/KURZZEIT wurde in der letzten Zeit erweitert um Modelle für Koaleszenz und zeitabhängigen Volumenausgleich bei intragranularen Blasen, für das Verhalten des intergranularen Gases und für die transiente Gasfreisetzung aus geschlossener Porosität. Das Modell wird beschrieben, und die Resultate einiger Vergleiche von Rechnungen und Experimenten werden diskutiert. Am Schluß wird ein Ausblick auf weitere notwendige Modellverfeinerungen gegeben.

Contents

1. Introduction

The behaviour of fission gases trapped in the fuel matrix is one of the important processes to be modeled in programmes used for fast reactor transient analysis. If present, these gases may play an important role in determining time and mode of fuel element failure for transient overpower and loss of flow accidents and may influence subsequent fuel motion. Therefore in past years efforts have been intensified to understand the physics of fission gas behaviour under steady state and transient conditions. In a number of papers the influence of fission gases on the different phases of accidents has been assessed /1-3/ and codes were developed dealing with different aspects of fission gas behaviour /4-9,21/. At the same time, efforts at gaining an experimental basis for such codes were intensified, resulting in the recent and ongoing performance of various in- and out-of-pile transient experiments /10,11/.

Codes simulating transient fission gas behaviour must encompass a steady state model yielding the initial conditions at the start of a transient - quantity of intra- and intergranular gas in solution and in bubbles and gas in closed and open fuel porosity. The transient model must be able to simulate the release of gas from the interior of the grains, the grain boundaries, and the porosity, and the behaviour of gas in molten fuel. The interaction of such a model with those describing structure and mechanical behaviour of fuel elements results in estimates on fuel element failure and fuel motion as a function of the evolution of a transient. Among the various effects that may be caused by fission gases are fuel pin failure induced by gross fuel swelling or pressure of released gas, solid fuel disruption and dispersal, and frothing or foaming of melting or molten fuel.

The code used in Karlsruhe for explicitely modeling fission gas behaviour is called LANGZEIT/KURZZEIT . It has been in operation for some time /12,13/ and has recently been extensively remodeled to include intragranular bubble coalescence and time dependent volume equilibration, intergranular gas components and transient gas release from porosity /14/. In addition, its models have been tested on the newest experimental results available. In its present form, the model

subdivides the gas contained in solid fuel into three main components:

a. Intragranular gas. Partly, this gas is contained in intragranular bubbles, the rest is in solution in the fuel matrix.

b. Intergranular gas. Again, this gas is in part contained in lenticular bubbles and partly resolved in the grain boundary region.

c. Porosity gas. This is the gas gathering on grain edges and in pores which eventually interlink and vent. Most of it is contained in the closed porosity, but there is a small portion which pressurizes the open porosity.

There are a number of processes linking the components:

a. Precipitation of dissolved gas into the gas bubbles.

b. Resolution in the fuel matrix of precipitated gas; this process is caused by the collision of energetic fission fragments with the gas atoms.

c. Migration of dissolved gas to the grain boundaries and edges.

d. Migration of the gas bubbles to grain boundaries and edges; this process is activated at the higher temperatures associated with a transient and driven by a temperature gradient.

e. Interlinkage and venting of pores.

When the fuel reaches the melting point, the above model is replaced by a simple one calculating bubble buoyancy and coalescence in the viscous fluid.
The behaviour of intergranular gas has been treated with a great deal of sophistication in some of the models cited above /4-6/, which subdivide the bubbles into groups characterized by bubble volume and a disequilibrium parameter. Some simplified models have recently been published /9,15/. LANGZEIT/KURZZEIT is to be counted

among the simplified codes, since it is attempted to describe the main physical processes with a restricted number of equations. The intragranular bubbles are characterized by but one mean radius and one mean value of excess pressure; the intergranular bubbles are treated in the same way. A lot of detail is lost by this approximation, but this has been deemed tolerable considering the large uncertainties in material parameters and sometimes even physical models.
The following chapters will deal with the model assumptions and equations for the three components, intra- and intergranular and porosity gas, and the model for melting fuel. There follows a chapter on comparisons with recent experiments. It should be stressed here, that the present model is neither complete nor final and that work on it will have to continue for some time to come. Some remarks on the merits and deficiencies of the model and necessary future developments conclude the presentation.

2. Intragranular gas

The equations governing the behaviour of intragranular gas have been formulated for the very first version of LANGZEIT/KURZZEIT already /20/, but had to be reevaluated for the new version since the assumption of equilibrium gas bubble volume was abandoned. Therefore, the bubble radius could not be replaced in the equations by using the ideal gas law as was done in the old version, but turns up explicitely.
The gaseous fission products are created within the fuel matrix, where at the beginning of fuel life they accumulate and soon reach a state of supersaturated solution. They then start to precipitate into small intragranular bubbles that form at lattice defects caused, e.g. by fission spikes /16/. Collisions with energetic fission fragments cause resolution of the gas contained in the bubbles, and in addition the resolved gas may diffuse to the grain boundaries and edges. The balance equation governing these processes is /17/

$$\dot{c} = \beta - \dot{g} - \frac{dP}{dt} + \frac{dR}{dt} \qquad (1)$$

c concentration of resolved intragranular gas

β rate of gas formation by fission

g concentration of gas escaped from the grain

$\frac{dP}{dt}$ intragranular precipitation rate

$\frac{dR}{dt}$ intragranular resolution rate

According to Ham /18/, the precipitation rate by diffusion into spherical bubbles is

$$\frac{dP}{dt} = 4 \pi D_g c r n \qquad (2)$$

D_g diffusion constant of fission gas in the fuel matrix

r intragranular bubble radius

n number density of intragranular bubbles

For resolution one must take into account, that atoms hit in the middle of a bubble have a bigger chance of colliding with another atom and losing their energy before reaching the surface than atoms closer to the surface. According to Nelson /19/, this fact may be approximated as resolution taking place only in an outer shell of thickness d. For a single small bubble with radius $r \leq d$, resolution is simply given by

$$\frac{dR_b}{dt} = n_a \eta \qquad (3a)$$

$\frac{dR_b}{dt}$ resolution rate for a single bubble

n_a number of atoms in intragranular bubble

η number of hits per atom per sec leading to resolution, resolution parameter

whereas for a bubble with r>d, from simple geometry

$$\frac{dR_b}{dt} = n_a \eta \ \frac{3d}{r}\left(1 - \frac{d}{r} + \frac{1}{3}\frac{d^2}{r^2}\right) \qquad (3b)$$

d thickness of resolution shell
η, of course, is proportional to the fission rate which, in turn, is proportional to ß.

$$\eta = \eta_o \cdot \beta \qquad (4)$$

It should be noted here that there is a large uncertainty for this parameter /13/ (see chapter 6).

From the above formulas, resolution for the total amount of gas in bubbles is

$$\frac{dR}{dt} = b \cdot \eta \qquad r \leq d$$

$$\frac{dR}{dt} = b\ \eta\ \frac{3d}{r}\left(1 - \frac{d}{r} + \frac{1}{3}\ \frac{d^2}{r^2}\right) \qquad r \gtrsim d \qquad (5)$$

$$\frac{dR}{dt} = b \cdot \eta\ \frac{3d}{r} \qquad r >> d$$

with

$$b = n_a \cdot n = \int_o^t \beta\ (t')\ dt' - c - g \qquad (6)$$

$$= \beta t - c - g \qquad \text{for } \beta \text{ constant with time}$$

b concentration of gas in intragranular bubbles
t irradiation time

The quantity of gas escaping to the grain boundaries is calculated by evaluating diffusion of atomic gas in the spherical grain and is given by /20/

$$\dot{g} = \text{Pos}\ (\dot{c}) \cdot F(t) + c \cdot \dot{F}\ (t) \qquad (7)$$

with

$$\text{Pos}\ (a) = \frac{1}{2}\ (a+/a/)$$

$$F(t) = 1 - \frac{6}{\pi^2} \sum_i \frac{1}{i^2} \exp\left(- \frac{i^2 \pi^2 D_g t}{a^2} \right) \qquad (8)$$

a grain radius

So far, the equations were formulated without specifying either steady state or transient conditions. It is assumed for steady state, that irradiation conditions remain constant, i.e.ß and D_g do not change with time. In addition the number of bubbles is assumed to be a constant derived from post-irradiation examinations . Bubble volume is supposed to be in equilibrium with local pressure and to be governed by a Van-der-Waals equation

$$\frac{b}{n} R_g T = (\alpha r^3 - \frac{b}{n} w) \left(\frac{2\gamma \sin\psi}{r} + p \right) \qquad (9)$$

$\frac{b}{n}$ gas contents of one intragranular bubble in moles

R_g universal gas constant

w Van-der-Waals constant

γ surface tension of fuel

p local hydrostatic pressure

This equation has been given the generalized form suitable for lenticular bubbles. For spherical bubbles

$$\alpha = \frac{4\Pi}{3} \quad ; \quad \sin\psi = 1$$

It can be quickly solved for r by the following procedure:

$$r_o = \sqrt{\frac{bR_gT}{2\gamma\alpha n \sin\psi}} \tag{10}$$

$$r_1 = \sqrt[3]{r_o^3 \frac{2\gamma\sin\psi}{2\gamma\sin\psi + r_o p} + \frac{bw}{n\alpha}} \tag{11}$$

$$r_{i+1} = r_i - \frac{f(r_i)}{f'(r_i)} \qquad i \geq 1 \tag{12}$$

$$f(r) = \alpha r^3 (pr + 2\gamma\sin\psi) - \frac{b}{n}(r(R_gT + pw) + 2\gamma w\sin\psi)$$

with (12) constituting a Newton-Raphson procedure, (10) being derived from the ideal gas law and (11) forming a kind of Van-der-Waals correction to (10). In practice, (11) is mostly so good an approximation that but one Newton-Raphson iteration suffices to reduce the error below 10^{-4}.
The steady state procedure for intragranular gas thus consists of solving the two differential equations (1) and (7) for c and g, using the balance equation (6) for deriving b. A Runge-Kutta method with self-adjusting time step lengths is applied.

At higher irradiation temperature and longer irradiation times, i.e. at conditions typical for restructured fuel zones, intragranular gas concentrations tend to reach quasistationary conditions with only b depending weakly on external pressure. Then

$$\dot{b} = \frac{dP}{dt} - \frac{dR}{dt} \approx 0 \qquad (13)$$

is used instead of the differential equations to directly calculate end of irradiation conditions.

If a steady state calculation is followed by a transient, a distinction is made between accident simulation, for which conditions can be assumed to be identical at the end of the irradiation and the start of the transient, and simulation of experiments. Fuel used for transient experiments has usually experienced an intermediate cooling period and, possibly, relief of external pressure by cutting. Since bubbles tend to shrink to their new equilibrium volume during such a period /27/, the initial transient bubble radius is in this case taken to be the value at 300 ^{o}K and 1 Bar. Other intermediate models can be easily realized if necessary.
For steady state calculations, immobile intragranular bubbles are assumed. At low irradiation temperatures, i.e. those in the unrestructured zone, they are in fact practically immobile, and the picture used in LANGZEIT is correct. At higher temperatures, they move slowly /22/ and eventually reach the grain boundary, being replaced by new ones in the interior of the grain. Instead of modeling this process, LANGZEIT uses a suitable average bubble density. This simplification is acceptable, since it applies to zones that retain very little gas and thus are of little importance for overall transient gas behavior.

If during a transient higher temperatures and appreciable temperature gradients occur, bubble mobility is strongly increased. Bubbles start to move up the gradient /23/, coalesce and may be released to the grain boundary. Random migration occurs as well. Coalesced bubbles do not immediately attain equilibrium volume. Since these processes are modeled in KURZZEIT, the equations governing intragranular gas behaviour have to be modified.

Equations (1) and (7) together with (6) can be retained, if (8) is changed to accomodate a strongly temperature dependent diffusion coefficient D_g.
This is done by replacing t by $t' = \tau/D_g(o)$ with /12/

$$\tau = \int_0^t D_g(t)\, dt \; ; \qquad \tau = D_g(t) \tag{14}$$

In fact this entails solving a third differential equation. There are two additional differential equations for bubble density n and non-equilibrium bubble radius r.
For biased migration, the number of coalescences occuring in time interval Δt for two classes of bubbles with radius r_1, r_2, velocity r_1, r_2 and number density n_1, n_2 is /24/

$$G_{1,2} = n_1 n_2 \, \Pi \, (r_1+r_2)^2 \, / \, v_1-v_2 \, / \, \Delta t \tag{15a}$$

Similarly for random migration with bubble diffusion coefficient D_{b1}, D_{b2}

$$G_{1,2} = n_1 n_2 \, 4\Pi \, (D_{b1}+D_{b2}) \, (r_1+r_2) \, \Delta t \tag{16a}$$

Somehow, these formulas have to be approximated, since KURZZEIT accomodates but one class of bubbles. Assuming that the mean difference of bubble velocities is proportional to the mean bubble velocity, we approximate (15a) and (16a) by

$$G_{biased} = \frac{n^2}{2} \; 4\Pi r^2 v \; C_1 \, \Delta t \tag{15b}$$

$$G_{random} = \frac{n^2}{2} \; 16\Pi D_b \, r \, C_2 \, \Delta t \tag{16b}$$

with the correction factors C_1 and C_2 taking into account the actual size distribution.

Using

$$v = \frac{4\Pi r^3 D_b Q_s \nabla T_s}{3\Omega k T^2} \qquad (17)$$

v Velocity of intragranular bubbles

D_b diffusion coefficient of intragranular bubbles

Q_s surface-diffusion heat of transport

∇T_s thermal gradient at bubble surface

k Boltzmann constant

Ω molecular volume

for the bubble velocity due to surface migration in a temperature gradient /15/ and

$$D_b = \frac{3\nu\Omega^2 D_s}{2\Pi r^4} \qquad (18)$$

ν surface density of diffusion atoms = $\Omega^{-2/3}$

D_s surface diffusion coefficient

one gets for the decrease of bubble number density due to coalescence by biased and random migration:

$$\frac{dn}{dt} = \frac{4\Pi\nu\Omega r n^2 D_s Q_s \nabla T_s}{kT^2} C_1 + \frac{12\nu\Omega^2 n^2 D_s}{r^3} C_2 \qquad (19)$$

For the thermal gradient at the bubble surface, according to /25/

$$\nabla T_s = \frac{3}{2} \nabla T$$

∇T bulk thermal gradient

A simplified approach similar to the one-bubble-class treatment of LANGZEIT/KURZZEIT has recently been made /1o/ using numerical results from the more sophisticated code FRAS2 /5/ to derive correction factors. A comparison with the formulas given by Cano et al. /10/ yields

$$C_1 = \frac{1}{2}\left(1.61 - 2.49\,\frac{pr}{3pr+4\gamma}\right) \qquad (21)$$

$$C_2 = 1.6$$

During a transient changes in external pressure and fuel temperature normally take place so fast that bubble volume cannot immediately be adjusted to its equilibrium value. In addition, onset of bubble coalescence furthers the disequilibrium. This fact can be easily illustrated by assuming the ideal gas law holds. At zero external pressure, the equilibrium radius for a bubble containing n_a atoms is

$$r = \sqrt{\frac{3n_a kT}{8\pi\gamma}}$$

If two such bubbles coalesce, the equilibrium radius for the product bubble containing $2n_a$ atoms is

$$r_{eq} = \sqrt{2r}$$

On the other hand, the initial volume of the product bubble before the onset of compensating processes is but the sum of the volumes of the two separate bubbles i.e.

$$r_{n.e.} = \sqrt[3]{2r}$$

The bubble volume after coalescence is thus smaller than the equilibrium value.

Growth of the bubble radius in the present model is controlled by three processes: coalescence, net diffusion of resolved gas with 1-2 vacancies per atom into the bubble, and diffusion of vacancies to the bubbles, which relieves the excess

pressure caused by non-equilibrium. The rate of change in bubble radius is thus the sum of three components:

$$\dot{r} = \dot{r}_{co} + \dot{r}_{yd} + \dot{r}_{dc} \qquad (22)$$

The change of bubble radius due to coalescence can be deduced from the conservation of total bubble volume at coalescence:

$$\frac{d}{dt}(nr^3) = 0$$

$$\dot{r}_{co} = -\frac{r}{3}\frac{\dot{n}}{n} \qquad (23)$$

The resolved gas diffuses in the lattice mainly by occupying vacancies /26/ and thus, when precipitated into the bubbles, causes a small volume increase. For a time interval Δt it is given by

$$V(t+\Delta t) = V(t) + \frac{dp}{dt}\Delta t \frac{\Omega L}{n} \qquad (24)$$

L Loschmidt number

From this

$$\dot{r}_{gd} = \frac{\Omega L}{4\Pi r^2 n}\frac{dp}{dt} \qquad (25)$$

Volume equilibration by vacancy diffusion has recently been included in models for intragranular gas bubble behaviour by several authors /5,6,21,28/, and is treated using the analysis by Greenwood et al /26/.

According to Greenwood et al. and neglecting the effects of vacancy depletion

$$\dot{r}_{dc} = \frac{D_u \Omega P_{ex}}{rkT}\frac{r_z}{r_z - r} \qquad (26)$$

D_u self diffusion coefficient of uranium in grain

P_{ex} excess pressure in bubble

$2r_z$ mean distance between bubbles

$$r_z = \sqrt[3]{r^3 + \frac{3}{4\pi n}} \qquad (27)$$

From the Van-der-Waals equation with w=0, i.e. sufficiently large bubbles

$$P_{ex} = \frac{2\gamma}{r^3}(r_{eq}^2 - r^2) + \frac{p}{r^3}(r_{eq}^3 - r^3) \qquad (28)$$

r_{eq} equilibrium bubble radius

At the moment, with no model for calculating external pressures and strains p=0 is assumed. Thus, finally

$$r_{dc} = \frac{2\gamma D_u \Omega}{r^4 kT} \cdot \frac{r_z}{r_z - r}(r_{eq}^2 - r^2) \qquad (29)$$

With these equations, the system of differential equations to be solved for the simulation of transient intragranular gas behaviour is completed. It is again solved with a Runge-Kutta-method. The transient equations for intergranular and porosity gas are treated separately and are coupled to those for the intragranular gas by the sources of gas released to the grain boundaries and edges. Since average values per time step are used for presenting such sources, the time steps must be sufficiently small. At the moment, the choice of intervals is up to the user with the programme issuing recommendations for a shortening of steps if necessary. An automatic shortening routine and better coupling, e.g. via linear functions instead of averages can be easily envisaged.

At the end of this chapter, the treatment of gas release to the grain surface and the different ways of coupling intra- and intergranular gas components in the steady state and transient model are described. For reasons given above, steady state intragranular gas release is effected solely by the diffusion of resolved gas atoms to the grain boundaries, i.e. is given by g. The coupling of intra- and intergranular models is done directly by simultaneously solving the respective equations.

In the transient part, the contribution of the resolved gas is taken into account, but is mostly of little importance compared to the release by bubble migration. The fraction of gas bubbles released to the grain boundaries during a transient is calculated using the model of Gruber /15/, which assumes that all bubbles move with the same velocity in the same direction across the spherical grain. With the time dependent velocity v(t) given by (17), the total distance traveled by a bubble during a transient is

$$s(t) = \int_0^t v(t')\, dt'$$

s distance traveled by a bubble during transient

From simple geometry considerations, the fraction of bubbles that has reached the boundary till time t is (see fig. 1) /15/

$$F_R = \frac{s}{4a}\left(3 - \frac{s^2}{4a^2}\right) \qquad s \leq 2a \qquad (30)$$

$$= 1 \qquad s > 2a$$

F_R release fraction of intragranular bubbles

From the values of g, F_R, b, n and r at start and end of a transient time interval, the quantity of gas arriving at the grain surface as well as mean radius and gas content of the released bubbles are calculated. These values are used as input to the programme part describing transient intergranular gas behaviour.
Steady state and transient intragranular swelling is calculated by simply summarizing the volume of all bubbles, taking into account the release fraction. Thus

$$S = \frac{4\Pi}{3} r^3 n (1 - F_R) \qquad (31)$$

width $F_R = 0$ for steady state.

S intragranular swelling

3. Intergranular gas

Since intergranular modeling is in many aspects similar to the intragranular model, the same notation is used as far as possible with an asterisk denoting intergranular quantities.
Some of the ideas for modeling grain boundary gas have been developed by Markworth already /29/. Gas arriving at the surface during steady state irradiation diffuses into grain boundary bubbles. These have been shown to be lenticular bubbles /30/(fig.2)with contact angle Ψ. Recent theoretical investigations have established /31-33/ that the bubbles tend to be uniformly spaced and of equal size, and that there is a maximum covering of grain surface, beyond which interlinkage and venting occurs. These results have been built into the model.
First, a few geometric relations must be given. Part of the grain surface is directly in contact with the closed or open porosity, and gas escaping through this part of the surface does not contribute to the intergranular component. If one assumes that one grain has 12 neighbours, the contact surface containing the intergranular gas can be idealized as 12 identical plane circles. The radius of this idealized grain boundary is

$$a^* = a\sqrt{\frac{1-dO}{3}} \qquad (32)$$

a^* grain boundary radius

dO fraction of grain surface in contact with porosity

d_O is assumed to be independent of time.
The intergranular bubble density n^* is taken to be a surface density and is related to the volume density by

$$n^*_{vol} = \frac{3}{2a}\,(1 - dO)\,n^* \qquad (33)$$

n^*_{vol} Volume density of intergranular bubbles

n^* surface density of intergranular bubbles

If the lenticular bubbles are characterized by their radius r^* and contact angle Ψ (fig.2), the following relations hold:

bubble volume: αr^{*3} ; $\alpha = \frac{2\Pi}{3} \frac{(1-\cos\Psi)\ (2+\cos\Psi)}{\sin\Psi\ \ (1+\cos\Psi)}$ (34)

bubble surface: $\frac{4\Pi r^{*2}}{1+\cos\Psi}$ (35)

radius of curvature: $\frac{r^*}{\sin\Psi}$ (36)

r^* radius of intergranular bubbles.
Ψ contact angle of intergranular bubbles

The intergranular gas is split into three components as was done for the intragranular gas. The balance equation governing them is

$$c^* + b^* + g^* = (1 - dO)\ (g + bF_R) \tag{37}$$

c^* intergranular resolved gas
b^* intergranular gas in bubbles
g^* gas escaped from boundary

For steady state, the number of bubbles is assumed to be a known constant and the bubble radius to have its equilibrium value given by (19). We then need two equations in addition to (37) for calculating the three components. The balance equation for the resolved intergranular gas is

$$\dot{c}^* = \dot{g}\ (1 - dO) - \frac{dP^*}{dt} + \frac{dR^*}{dt} - \dot{g}^* \tag{38}$$

$\frac{dP^*}{dt}$ intergranular precipitation rate

$\frac{dR^*}{dt}$ intergranular resolution rate

One could expect the precipitation model to be a two-dimensional equivalent of the intragranular model, if c^* could be figured to result only from intragranular gas release. However, gas resulting from intergranular resolution has to be accounted for in addition. This was indicated by a first estimate, which showed intergranular resolution to have an importance comparable to intragranular resolution. In a first attempt, the intergranular resolution component was added to the intragranular resolved gas. This resulted in an unacceptably small steady state gas release, which was in total disagreement with experimental results. Therefore, it is reasoned that the intergranular resolution component remains in the vicinity of the boundary and eventually diffuses back to the intergranular bubbles. c^* is therefore taken to result from both intragranular release and intergranular resolution, as is indicated in (38) already. The model used for precipitation is therefore a three-dimensional one, incorporating the outer grain regions.
Again, the model developed by Ham /18/ is employed. His results, for gas precipitated into a spherical bubble from a surounding spherical shell is

$$\frac{dP^*}{dT} = \frac{c^* \; 3r^*_{eff}}{r^*_z} \; D_g$$

r^*_{eff} radius of spherical bubble

r^*_z radius of spherical cell

The lenticular bubbles are idealized as spherical with identical volume, resulting in an effective radius

$$r^*_{eff} = \sqrt[3]{\frac{3\alpha}{4\pi}} \; r^*$$

The cell radius is derived from the spacing of the intergranular bubbles:

$$r^*_z = \frac{1}{\sqrt{\Pi n^*}}$$

With these assumptions

$$\frac{dP^*}{dt} = r^* c^* D_g \sqrt{\Pi n^*}^3 \quad 3 \cdot \sqrt[3]{\frac{3\alpha}{4\Pi}}$$

The assumptions made above are provisional ones that may be subject to further alterations. With a contact angle of 50° employed at the moment, the idealization of the lenticular bubbles as spherical can be tolerated, but if there is evidence of a much smaller angle, this assumption will hold no longer. The radius of the precipitation cell is really a planar value for the grain boundary only, and should be substantiated or modified by an estimate on resolution depths and diffusion lengths of the resolution component. For the diffusion, the intragranular value is employed at the moment. There is experimental evidence /50/, that gas diffusion is greatly enhanced in the grain boundary, but measured values vary appreciably. On the other hand, most gas undergoing resolution is transfered into the lattice near the bubble and only a small fraction into the boundary. Thus, the bulk of the resolved grain boundary gas will indead be governed by lattice diffusion. With more reliable values for grain boundary diffusion becoming available, a composite diffusion coefficient may be employed. Resolution is modeled in the same way as for intragranular bubbles, taking into account the different geometry. Thus, similar to (5):

$$\frac{dR^*}{dt} = b^* \eta \qquad r^* \frac{1-\cos\psi}{\sin\psi} \leq d$$

$$\frac{dR^*}{dt} = b^* \eta \left(1 - \sqrt{1 - \frac{2}{\sin\Psi}\,\frac{d}{r^*} + \frac{d^2}{r^{*2}}}\right)^3 \qquad (40)$$

$$r \frac{1-\cos\Psi}{\sin\Psi} \gtrsim d$$

$$\frac{dR^*}{dt} = b^* \eta \frac{3d}{r^* \sin\Psi} \qquad r \frac{1-\cos\Psi}{\sin\Psi} >> d$$

Release of gas from the boundary by diffusion to the edges is calculated in the same way as intragranular release. The difference is in geometry, with the spherical grain being replaced by a circular plane. The resulting equations are similar to (7) and (8), with $i\Pi$ being replaced by the zeros of the zero'th order Bessel-function.

$$g^* = Pos(\dot{c}^*) \cdot F^* + c^* \dot{F}^* (t) \qquad (41)$$

$$F^*(t) = 1 - 4 \sum \frac{1}{x_i^2} \exp\left(- \frac{x_i^2 D_g t}{a^{*2}}\right) \qquad (42)$$

x_i Zeros of zero'th order Bessel-function.

Eq. (41) and (38) together with (37) are sufficient for describing steady state intergranular gas behaviour. In the programme, (41) and (38) are combined with (1) and (7) for simultaneous solution in the steady state part. (6) and (37) are then used for calculating the remaining components.
So far, steady state percolation has not been accounted for.
If the maximum fraction of grain surface to be covered by bubbles without percolation is given, the maximum allowable bubble radius is

$$r^*_{Max} = \sqrt{\frac{B_{Max}}{\Pi n^*}} \qquad (43)$$

B_{Max} maximum fraction of grain boundary covered with bubbles

r_{Max} maximum bubble radius

If (43) is inserted into (9) and the resulting equation resolved for b, taking into account (33), the maximum concentration of gas contained in intergranular bubbles results:

$$b^*_{Max} = \frac{(1-dO)\ 3n^* \alpha r^{*3}_{Max}}{2a} \cdot \frac{2\gamma \sin\Psi + p r^*_{Max}}{2\gamma w \sin\Psi + r^*_{Max}\ (R_g T + pw)} \qquad (44)$$

b^*_{Max} maximum intergranular gas concentration of gas in bubbles

During steady state calculations, if b^* exceeds b^*_{Max}, it is reduced to b^*_{Max} and the difference added to g^*. This is done at the end of each time interval, but for consistency during the integration of the differential equations, b^* and r^* in (39) and (40) are reduced to their maximum values as well whenever they exceed them. The resulting population of reduced bubbles is an approximation of the real situation, in which continuous formation, movement, interlinkage, venting and sintering of bubbles occurs /32/.

As in the case of intragranunlar gas, intergranular gas concentrations may reach quasistatic conditions at higher irradiation temperatures and longer times. Then, b^* has reached its maximum value and is the only weakly time dependent component. In this case, (44) is used to calculate directly the condition at the end of the irradiation.

Conditions at the start of a transient are modeled in the same way as those for intragranular gas. For an accident simulation, the bubble radius at the end of the irradiation is retained, whereas for experiment simulation it is given the equilibrium value at 300^oK and 1 Bar.

The transient model is again in many respects similar to the intragranular one. Resolution, precipitation, and gas diffusion to the edges are retained from the steady state model. In addition, bubbles start to move at higher temperatures in the direction of the projection of the temperature gradient onto the plane /10/. Coalescence occurs in addition to percolation and bubbles are lost to the edges. On the other hand, their number is augmented by those arriving from the interior of the grain. Bubble volume is non-equilibrium, and equilibration by vacancy diffusion is accounted for. Eq.s(38) and (41)can be retained with small additions if, as for intragranular gas, (42) is changed to accomodate a strongly temperature dependent diffusion coefficient. Thus, eq. (14) is again added to the set of equations. Actually, (38) is replaced by the equation for b^* in the transient formulation

$$\dot{b}^* = \frac{dP^*}{dt} - \frac{dR^*}{dt} + Q - S_b \qquad (45)$$

Q_b rate of released intragranular gas adding to intergranular bubbles

S_b rate of intergranular gas released to edges by bubble migration

As is evident from the last term in this equation, gas release by migration is included in the differential equations. Percolation is not included, but is treated as in the steady state model. Some consideration has been given to the treatment of the intergranular bubble population evolving during a transient. When released intragranular bubbles start arriving on the grain boundary, part of them directly hits the intergranular bubbles and coalesces; the rest forms new intergranular bubbles, that add to the original population. The approximation, that first comes to mind for treating the resulting mixed population while retaining the concept of but one class of bubbles, is the use of averaged parameters. However, inspection of intragranular and intergranular bubble parameters in unrestructured zones quickly yields arguments against this approximation. At the start of a transient, the number of atoms per intragranular bubble may be more than a factor 100 smaller than that per intergranular bubble. On the other hand, the intragranular bubble number density may be four orders of magnitude bigger.
Thus if but 1% of the intragranular bubbles is released, there are about 100 times more small bubbles on the grain boundary than big ones. On averaging parameters, the big bubbles would completely disappear. Conditions change during the course of a transient. Then, due to temperature increase, coalescence and volume equilibration, the intragranular bubble volume grows and the number density shrinks to become more comparable to intergranular values, which do not change as fast. Thus, while averaging bubble parameters may be envisaged for later stages of a transient, it may unduly falsify the picture at the start. On the other hand, treating different classes of intergranular bubbles is undesirable for a simple code.
When the released intragranular bubbles are much smaller than the intergranular ones, their velocity in the temperature gradient is much bigger. Thus, they can be expected to eventually coalesce with the original intergranular bubbles. Assuming instantaneous coalescence

in one possible approximation to this behaviour. An approximation deemed more appropriate is to add the gas contents of the small bubbles to the resolved intergranular gas. Thus, a time lag for coalescence is realized while retaining the one group picture. This approximation is used until the size of released intragranular bubbles becomes comparable to that of the intergranular ones. Then, the use of the averaged parameters is adequate. For this reason, the ratio of gas atoms per intragranular bubble to that per intergranular bubble is examined during the course of a calculation. If this ratio is below a given limit, the gas contents of newly arriving bubbles, that do not hit an old bubble, is added to the resolved gas. If it exceeds the limit, the newly arriving bubbles, that do not coalesce, are added to the old population, averaging parameters. The "cut-off" limit is currently .2. Variation of the value by a factor of 2 in either direction does not appreciably influence the results.
As a further simplification, the intragranular gas released by diffusion is added to the released bubbles, i.e. is treated as if it were contained in bubbles. The error is not noticeable, since this contribution is several orders of magnitude smaller in transients than the release by bubble migration.
With these approximations, Q_b from (45) is given by the following formulas:

$$Q = (1-dO)\,\frac{d}{dt}\,(bF_R + g) \qquad (46)$$

Q rate of gas released to boundaries

$$B = \Pi n^* (r^* + r)^2 \; ; \quad \text{if } B > 1 \text{ , } B = 1 \qquad (47)$$

B probability for released intragranular bubble to hit intergranular bubble

$$\begin{aligned} Q_b &= Q \cdot B \quad \text{if} \quad n_a/n_a^* < L_c \\ Q_b &= Q \quad \text{if} \quad n_a/n_a^* \geq L_c \end{aligned} \qquad (48)$$

n_a^* number of gas atoms per intergranular bubble

L_c cut-off limit for averaging intergranular bubble parameters

Next, bubble migration must be treated. First, the bubble diffusion coefficient due to surface diffusion is evaluated by simply extending the analysis by Gruber /34/ for spherical bubbles to the boundary bubble geometry. The result is

$$D_b^* = \frac{4\Pi\nu\Omega^2 D_s}{(1+\cos\Psi)\alpha^2 r^{*4}} \qquad (49)$$

D_b^* diffusion coefficient of lenticular bubble.

Then, again following closely the derivation by Gruber /15/ and assuming a mean angle between temperature gradient and boundary of 45^o, the bubble velocity is calculated as

$$v^* = \frac{4\Pi\nu\Omega D_s Q_s \sin 45^o \nabla T_s}{(1+\cos\Psi)\ \alpha r^* kT^2} \qquad (50)$$

v^* intergranular bubble velocity

The model for release by migration of intergranular bubbles is in part a two-dimensional equivalent of the intragranular one. First, fig. 1 is again used with the circles now representing the idealized boundary.
From simple geometry, the release fraction is

$$F_R^* = \frac{2}{\Pi} \arcsin\frac{s^*}{2a^*} + \frac{s^*}{\Pi a^{*2}}\sqrt{a^{*2} - \frac{s^{*2}}{4}} \qquad s^* \leq 2a^*$$

$$F_R^* = 1 \qquad s^* > 2a^* \qquad (51)$$

s^* distance traveled by intergranular bubble during the transient

F_R^* fraction of intergranular bubbles released by migration.

Actually, the picture does not quite describe the situation, because as an important difference to the intragranular case the space voided from original bubbles can be filled up with released intragranular bubbles. Thus, an approximately even distribution of bubbles over the whole area of the boundary is kept up a long time during the release process. One may therefore approximate the differential release fraction by its initial value, i.e.

$$\frac{dF_R^*}{dt} = \frac{dF_R^*}{ds^*} \quad \frac{ds^*}{dt} = \frac{dF_R^*}{ds^*}\Bigg|_{s^*=0} \cdot \quad v^* = \frac{2v^*}{\Pi a^*} \qquad (52)$$

The error introduced by this approximation is not very big, since most gas release from boundary bubbles is by percolation, as has been remarked by Cano et al. /10/ already and was evidenced by KURZZEIT-results. A bigger error may only result in fuel regions containing little gas and, consequently, no percolation; such zones contribute little to the overall fission gas effect and thus need not be modeled exactly.

With (52), the rate of gas release by bubble migration is

$$S_b = \frac{2}{\Pi} \frac{v^*}{a^*} b^* \qquad (53)$$

This term turns up in (45) and also must be added to the equation describing gas release. Thus, the steady state equation (41) is to be replaced by, for the transient

$$\dot{g}^* = \text{Pos}\ (\dot{c}^*)\ F^*(t) + c^*\ \dot{F}^*(t) + S_b \qquad (54)$$

The transient change in bubble density is a sum of three components: a decrease due to coalescence, an increase due to released intragranular bubbles, that do not merge with an intergranular one, and a decrease due to migration to the edges.

Thus:

$$n^* = n^*_{co} + n^*_{re} + n^*_{mi} \qquad (55)$$

Coalescence is calculated in the same way as for intragranular bubbles, taking into account the plane geometry. Instead of (15a), the number of coalescences in time interval Δt for two classes of bubbles with radii r_1^*, r_2^*, velocities v_1^*, v_2^*, and number densities n_1^*, n_2^*, is now given by

$$G^*_{1,2} = n_1^* n_2^* (2r_1^* + 2r_2^*) \left| v_1^* - v_2^* \right| \Delta t \qquad (56)$$

This is approximated by

$$\dot{n}^*_{co} = -\frac{n^{*2}}{2} 4r^* v^* C_3 \qquad (57)$$

with C_3 taking into account the effect of the actual size distribution. By introducing (50):

$$\dot{n}^*_{co} = \frac{8\Pi \sin 45^o}{(1+\cos\Psi)\ \alpha} \cdot \frac{n^{*2} \nu\Omega\ D_s\ Q_s\ \nabla T_s}{kT^2} \quad C_3 \qquad (58)$$

An evaluation of the correction factor is difficult, since the original bubbles tend to have similar sizes, thus requiring a small correction factor. When intragranular bubbles start to arrive, the size distribution becomes less uniform and the correction factor grows. A comparison with the results of Cano et al /10/, who estimated the factor for a population of only the released intragranular bubbles, yields C_3=.5. No further investigation was made so far, and a tentative value of .5 was postulated.
The second contribution to the change in bubble density is found by stating, first, that the number of bubbles arriving at the grain boundary per unit time, Q_n, is related to the rate of gas released, Q from (46), by

$$Q_n = Q \cdot \frac{n}{b}$$

The fraction B (see (47)) of these merges with intergranular bubbles, whereas the fraction (1-3) forms new bubbles. Taking into account the cut-off limit explained above, and transforming to a bubble density per unit area via (33), one arrives at

$$\dot{n}^*_{re} = 0 \qquad n_a/n^*_a < L_c$$

$$\dot{n}^*_{re} = \frac{2}{3}\, a\, (1-B)\, \frac{n}{b}\, \frac{d}{dt}\, (bF_R+g) \qquad n_a/n^*_a \geq L_c \qquad (59)$$

The loss of bubbles by migration is, analogous to (53):

$$\dot{n}^*_{mi} = -\frac{2}{\Pi}\, \frac{v^*}{a^*}\, n^* \qquad (60)$$

This last term is, in addition to its contribution to (55), integrated seperately, because it is needed later for calculating the transient growth of porosity.
The change in bubble radius is given by four components, three of which are similar to those for intragranular bubbles (see eq. (22)):

$$\dot{r}^* = \dot{r}^*_{co} + \dot{r}^*_{gd} + \dot{r}^*_{dc} + \dot{r}^*_{re} \qquad (61)$$

They are due to, respectively : Coalescence with other intergranular bubbles, vacancies associated with precipated gas, diffusion of vacancies and addition of released intragranular bubbles.
The change due to coalescence among intergranular bubbles is, as for the intragranular ones

$$\dot{r}^*_{co} = -\frac{r^*}{3}\, \frac{\dot{n}^*_{co}}{n^*} \qquad (62)$$

The increase of the radius due to vacancies associated with precipitated gas is (see. eq. (25))

$$\dot{r}^*_{gd} = \frac{\Omega L}{3\alpha r^{*2} n^*} \cdot \frac{2a}{3(1-dO)} \cdot \frac{dP^*}{dt} \qquad (63)$$

Vacancy diffusion consists of two components, namely vacancies diffusing along the boundary and those arriving from the inside of the grain. At first sight, one might be inclined to drop the lattice component, because the diffusion coefficient for this process is orders of magnitude smaller than that for boundary diffusion. One can then follow the analysis by Hull and Rimmer /35/, as has been done recently in an assessment of the ability of grain boundary bubbles to crack the fuel /36/, and calculate bubble growth in a planar model. The result is

$$\dot{r}^*_{dc,1} = \frac{(4\Pi)^2 \sin\Psi}{3\alpha} \cdot \frac{D^*_u \delta_z \Omega\gamma \sqrt{n^*}}{kTr^{*4}} (r^{*2}_{eq} - r^{*2}) \qquad (64)$$

D^*_u self diffusion coefficient of uranium in grain boundary

δ_z width of grain boundary

r^*_{eq} equilibrium intergranular bubble radius

Upon inspection of the diffusion coefficients found in literature (see table 1), one remarks that the value for lattice diffusion grows faster with temperature than the one for boundary diffusion. Table 1 gives, in addition, the boundary width and a typical radius of an intragranular bubble, i.e. the two values determining the contact area of the bubble with the boundary resp. lattice. A composite value for the self-diffusion coefficient would have to be

$$\bar{D}_u = \frac{D_u r^* + D^*_u \delta_z}{r^* + \delta_z}$$

It is obvious from this formula and the numerical values in table 1, that at higher temperatures the contribution of lattice diffusion cannot be neglected any more.

In chosing an appropriate model one must keep in mind, that the intergranular bubbles compete with the intragranular ones in attracting vacancies from the lattice. Therefore a spherical model for the intergranular bubbles employing a cell radius which is of necessity questionable and neglecting the strong anisotropy seems unsuitable. Rather, the contribution from lattice self-diffusion is treated separately:

$$\dot{r}^*_{dc} = \dot{r}^*_{dc,1} + \dot{r}^*_{dc,2} \qquad (65)$$

with the first term given by (64). For calculating the lattice term the model of Greenwood et al./26/, was extended to plane geometry with a cell width given by the mean distance between the bubble surface and the next neighbouring bubble. The result is

$$\dot{r}^*_{dc,2} = \frac{8\pi\sin\Psi}{3\alpha(1+\cos\Psi)} \cdot \frac{\gamma\Omega D_u}{kTXr^{*3}} \cdot (r^{*2}_{eq} - r^{*2}) \qquad (66)$$

X Cell width for vacancy diffusion from lattice to intergranular bubble

The cell width is derived from the following geometrical considerations. Taking intragranular swelling into account, the distance from an intergranular bubble across the grain is

$$L = 2a\ (1 + \frac{S}{3})$$

The mean distance across an intragranular bubble is

$$\ell = \frac{4}{3}\, r$$

and the mean number of intragranular bubbles sitting on a line across the grain can be derived from the swelling as

$$n = \frac{L \cdot S}{3\ell}$$

If n bubbles are randomly spaced on a line of length L, their mean distance from each other and from the end of the line is

$$2X = \frac{L - n\ell}{n + 1} \qquad (67)$$

Half of this distance is the cell width.
The change in mean radius by released intragranular bubbles that partly merge with the already existing intergranular bubbles and partly form new ones, is derived from the conservation of total volume.

$$\dot{r}^*_{re} = \frac{4\Pi/3 \cdot r^3}{3\alpha r^{*2} n^*} \cdot \frac{2a}{3} \frac{n}{b} \frac{d}{dt} (bF_R + g)$$

$$n_a/n_a^* < L_c$$

$$\dot{r}^*_{re} = - \frac{\dot{n}^*_{re}}{n^*} \cdot \frac{r^*}{3} + \frac{4\Pi/3 \; r^3}{3\alpha r^{*2} n^*} \cdot \frac{2a}{3} \frac{n}{b} \frac{d}{dt} (b F_R + g)$$

$$n_a/n_a^* \geq L_c \qquad (68)$$

The system of differential equations describing the transient behaviour of intergranular bubbles is thus completed and consists of eq. s (14), (45), (54), (55), (60), and (61), and the supplementary equations. It is solved with a Runge-Kutta-method.

As in the steady state case the bubble population may grow to cover more than the maximum allowable fraction of the surface and will then start to interlink and open up into the porosity. In this case, the programme calculates the excess number of bubbles, which is released. This is done every time the differential equations have been integrated over a given time interval. A recommendation for shortening the time steps may be issued by the code. The number of bubbles released by perlocation is given by

$$dn^* = n^* \frac{\Pi n^* r^{*2} - B_{Max}}{B_{Max}} \qquad \Pi n^* r^{*2} > B_{Max} \qquad (69)$$

$dn^* = 0$ otherwise

n^*, n^*_{mi}, b^* and g^* are modified with this value every time percolation takes place.

Intergranular swelling is the sum of all bubble volumes and, since losses are included in the definition of n^*, is simply

$$S^* = \alpha n^* r^{*3} \frac{2(1-dO)}{3a} \qquad (70)$$

S^* intergranular swelling

4. Porosity gas

Gas released from the boundaries gathers on the edges and in the fabricated porosity. With gas accumulating, the porosity starts to swell and eventually interlinks and opens. The gas is then released to the fission gas plenum and central void and contributes to the internal pressurization of the fuel element. During transients, the flow of gas from open porosity may be hindered by impermeable zones, e.g. melt fronts or zones, in which paths are closed under pressurization. Low fuel permeability may delay gas escape.

Steady state gas release from porosity has been modeled by Ronchi /17/ for LANGZEIT employing the percolation conditions derived by Maschke et al /37/. Here, the theory is only outlined.

Initially, the fuel contains closed pores, which are idealized as spheres with a given radius and number density. Their initial gas contents (fill gas) is calculated from the initial fuel element pressure using eq. (9). The additional gas arriving in a pore during irradiation is given by

$$q_p = g\ dO + g^* \tag{71}$$

With a given pressure rise during irradiation

$$p(t) = p_o + p_1 t \tag{72}$$

p_o initial fuel element pressure

p_1 change of fuel element pressure with time

the time dependent radius of the closed pores can be calculated from eq. (9), since there is enough time to reach equilibrium conditions. Using radii and number densities of pores and grains and an idealization of both as spheres, Ronchi then approximately calculates the average of bonds per pore from lattice geometry. Then the percolation condition of Maschke et al /37/ is applied,

which states that for

$$P_p > 1.569.... \qquad (73)$$

P_p number of bonds per pore

total interlinkage occurs. Actually, gas will not be released suddenly, when P_p reaches 1.569, but gradually when P_p approaches and exceeds this value, because the bonds are statistically distributed around the average values. The release fraction is therefore an integral of the form

$$F_p = \frac{1}{\sqrt{2\pi\delta}} \int_{1.569}^{\infty} \exp\left(-(x-P)/2\delta^2\right) dx \qquad (74)$$

F_p release fraction from pores

where δ is evaluated from experimental histograms of pore and grain radii and fractional porosity. From F_p, the fission gas contents of open and closed porosity follows as

$$b_p = q_p (1-F_p) + b_o F_p \; ; \qquad b_p \leq q_p \qquad (75)$$

b_p gas concentration in pores

b_o gas concentration in 100% open pores

For calculating the gas contents of open pores it is assumed, that due to sintering they achieve a given mean radius; from this and the external pressure, the gas contents is calculated by again employing eq. (9).

Transient release is up to now not fully modeled; there is, especially no model for the delay of release by low fuel permeability or blockages. Thus, release is assumed to be instantaneous upon opening of the pores. The fraction of open pores is calculated with Ronchi's model, but assuming non-equilibrium pore growth. Pore structure at the start of a transient is assumed to remain at its end of irradiation conditions.

The volume of open and closed porosity is assumed to grow due to addition of released intra- and intergranular bubbles and vacancies associated with released resolved gas. Each pore receives the same amount of gas, regardless of whether it is closed or open. Closed porosity grows, in addition, by vacancy diffusion. The increase in radius is written as

$$\dot{r}_x^* = \dot{r}_{x,gd} + \dot{r}_{x,\,re} + \dot{r}_{x,\,dc} \qquad (76)$$

with x standing for either c : closed, or o : open
For both types of porosity (see eq. (25)).

$$\dot{r}_{x,\,gd} = \frac{\Omega L}{4\pi n p r_x^2} \frac{d}{dt} (gdO + \tilde{g}^*) \qquad (77)$$

n_p number density of all pores

r_c radius of closed porosity

r_o radius of open porosity

$\tilde{g}^*$ is the intergranular gas released by gas diffusion only and is related to g^* from the foregoing chapter
by

$$\dot{\tilde{g}}^* = \dot{g}^* - \frac{b^*}{n^*} \dot{n}^*_{mi} \qquad (78)$$

The second contribution is, again for closed and open porosity (see. eq. (68))

$$\dot{r}^*_{x,re} = \frac{r^3 dO}{3 n_p r_x^2} \frac{n}{b} \frac{d}{dt} (bF_R) + \frac{\alpha r^{*3}}{4\pi n_p r_x^2}$$

$$\cdot \frac{3(1-dO)}{2\alpha} \dot{n}^*_{mi} \qquad (79)$$

The contribution of vacancy diffusion is (see. eq. (29))

$$\dot{r}_{c,dc} = \frac{2\gamma D_u \Omega^*}{r_c^4 \, kT} \left(r_{c,eq}^2 - r_c^2\right) \qquad (80)$$

$$\dot{r}_{o,dc} = 0$$

$r_{c,eq}^2$ equilibrium radius of closed porosity

If closed poresinterlink, the new average radius of open porosity is calculated from old and new value of the porosity release fraction with

$$r_{o,new}^3 = \frac{1}{F_{p,new}} \left(F_{p,old} \, r_{o,old}^3 + (F_{p,new} - F_{p,old}) \, r_c^3\right) \qquad (81)$$

Porosity swelling is not calculated for steady state. For the transient, swelling is the increase in pore volume given by eq.s (77), (79) and (80). Total swelling is then the sum of intra- and intergranular and porosity swelling.

5. Gas release upon melting

On melting, fission gas bubbles contained in the fuel may expand, coalesce, and ultimately cause fuel foaming and frothing. No modeling of the frothing process itself is attempted, but the time span until its onset is estimated. Before setting up the model, two time constants were evaluated to find out, what kind of processes must be simulated.
The first one concerns the time needed for an overpressurized bubble to reach equilibrium volume under the assumption, that the constraints posed by the solid fuel are removed instantaneously. The time dependence of bubble growth in a fluid is governed by the Navier-Stokes-equation, which for a spherical bubble may be reduced, similar to the derivation by Dalle Donne and Ferranti/38/, to the equation

$$\ddot{r}r + \frac{3}{2}\dot{r}^2 + 4\frac{\mu}{\rho}\frac{\dot{r}}{r} = \frac{p_{ex}}{\rho}$$

μ viscosity of molten fuel
ρ density of molten fuel

with initial conditions

$$r(0) = r_o \quad ; \quad \dot{r}(0) = 0$$

and

$$p_{ex} = \frac{\nu R_g t}{4\Pi/3 \cdot r^3} - \frac{2\gamma}{r} - p$$

This equation was solved using the Runge-Kutta-method for typical initial conditions derived from KURZZEIT-results and widely varying hydrostatic pressures. The resulting time constants are 10^{-6} - 10^{-8} sec. Thus, the volume equilibration process is so fast, that it can be assumed to be instantaneous.

Bubble movement in the fluid is assumed to be influenced by buoyancy and viscosity. Assuming laminar fluid flow arround the rising bubble, the equilibrium velocity is calculated from Stokes' law as /39/

$$v = \frac{2r^2 a_g}{9\kappa} \qquad (82)$$

a_g acceleration of gravity

κ kinematic viscosity of fluid fuel

The time needed for accelerating from zero velocity up to a fraction f of the equilibrium value is /39/,

$$t = \frac{2r^2}{9\kappa} \, lu \, \frac{1}{1-f}$$

For the biggest bubble radii resulting from KURZZEIT calculations ($3 \cdot 10^{-4}$cm), a time span of $5 \cdot 10^{-6}$ sec is calculated for reaching 90% equilibrium velocity. Again, this time is so small that instantaneous equilibrium velocity can be assumed.
Due to the small initial bubble radius, the Reynolds'number is so small, that Stockes'law is indeed valid.
When evaluating conditions near melting temperature as calculated by KURZZEIT for different transients, one finds that intra- and intergranular bubbles with widely differing parameters may remain in the fuel. The porosity has fully interlinked and vented with very little residual gas remaining. Therefore, porosity gas is not accounted for, though this may become necessary in the future, when a model for the pressurization of porosity is included.
It is not difficult to enlarge the model sketched below from two to three groups of bubbles in such a case.

The present model takes into account the following processes:

a. Up to two bubble groups (one only, if intragranular bubbles have been totally released), each of which has its own parameters and is individually released.

b. Coalescence of bubbles in one group with members of the same or the other group.

c. Formation of resolved gas by fission, precipitation and resolution.

One bubble group is fully characterized by its gas contents and number density. Bubble release is not included in the differential equations but treated at bigger time intervals as was done for intergranular gas. The differential equations describing the system are, analogous to those of intragranular bubbles in solid fuel

$$\frac{dn_1}{dt} = - G_{11} - G_{12}$$

$$\frac{db_1}{dt} = -G_{12} \frac{b_1}{n_1} + \frac{dP_1}{dt} - \frac{dR_1}{dt} \qquad (83)$$

$$\frac{dn_2}{dt} = - G_{22} \qquad (84)$$

$$\frac{db_2}{dt} = G_{12} \frac{b_1}{n_1} + \frac{dP_2}{dt} - \frac{dR_2}{dt}$$

n_i number density of bubbles in group i

b_i gas concentration in bubbles of group i

G_{ik} rate of coalescence for bubbles of group i with bubbles of group k

It has been assumed for this formulation, that the bubbles of group 1 are much smaller than those of group 2. Thus if two bubbles of group 1 coalesce, the resultant bubble remains in group 1, whereas for all other coalescences, the resultant bubble is in group 2 . - P_i, R_i are precipitation and resolution as given by eq.'s (2) and (5) with bubble radius r given by eq. (9) and the concentration of resolved gas c_m at time t into the melting process resulting from

$$c_m(t) = \int_0^t \beta dt + c + c^* + b + b^* - b_1 - b_2 \qquad (85)$$

c, c^*, b, b^* are the intra- and intergranular gas concentrations at onset of melting.

From eq.'s (15a, b) and (82), assuming the correction factor C_1 from eq. (15b) is 1. and the ideal gas law holds, the rate of coalescences results as

$$G_{ii} = 2\pi^2 b_i^2 \frac{a_g}{32\Pi_K} \frac{R_g^2}{\gamma^2} \qquad (86)$$

$$G_{ii} = \left(\frac{R_g T}{\gamma}\right)^2 \frac{g}{32\Pi_K} \left(\sqrt{\frac{b_1}{n_1}} + \sqrt{\frac{b_1}{n_2}}\right)^2 \left| b_2 n_1 - b_1 n_2 \right|$$

The system of equations may reduce to eq.'s (82) only with $G_{12} = 0$, if one group of bubbles is missing. This is the case if the intragranular bubbles have been fully released before onset of melting, if one group is released during melting, or if the radii of intra- and intergranular bubbles at onset of melting and after volume equilibration differ by no more than a factor of 2.
In this last case, the two types of bubbles are represented by one group with averaged parameters.

Eq.s (82) and (83) are integrated with a Runge-Kutta-method with automatic time step adjustment for a given time interval, This longer interval is used for calculating bubble release and is automatically reduced with growing bubble velocity.
Release for bubbles of group i is calculated from the distance the bubbles have traveled at time t into the melting process with their velocity given by eq. (82) and their radius resulting from eq. (9):

$$s_i(t) = \int_0^t \frac{2r_i^2(t)\, a_g}{9\kappa}\, dt \qquad (87)$$

From this, release is calculated as

$$F_i = \frac{s_i}{a_m} \qquad \text{if} \quad s_i \leq a_m \qquad (88)$$

$$= 1 \qquad \text{if} \quad s_i > a_m$$

a_m mean distance bubbles have to travel until release from melting or molten fuel

F_i release fraction for bubbles of group i

a_m is an input parameter, e.g. the fuel element diameter.
Swelling results from the above as

$$S_m = \frac{4\Pi}{3} \left(n_1 r_1^3 (1 - F_1) + n_2 r_2^3 (1 - F_2) \right) \qquad (89)$$

The calculation is finished if swelling exceeds 100%. At this value, neither Stokes' law nor the assumption of spherical bubbles is valid any more, and any further description would have to work with a two-phase-flow concept. This is not attempted, since it is beyond the framework of this code.

6. Results and conclusions

Before presenting the results of recent comparisons to experiments, some remarks must be made on the parameters used. Among the many parameters to be supplied to the code, some are of particular importance since results are quite sensitive to them, and knowledge is not always satisfactory. In 1977, the parameters were updated /13/, but that was before the inclusion of intragranular bubble coalescence and of the model for intergranular bubbles. Up to now, no further systematic evaluation was started, and parameters for the newly included models were taken from the available literature. The material data employed, save those specifying fabrication, irradiation and transient are listed in table 2 together with the relating literature. One must keep in mind, that LANGZEIT/KURZZEIT is, up to a degree, a parametric code, that can rightfully be made to fit experimental results by varying its parameters, but naturally only in some credible interval. Incidentally, one of the most sensitive parameters, the surface diffusion coefficient, which decisively influences transient gas release, has remained the same, though bubble coalescence was included.

The only appreciable parameter variation was necessitated by a change in the resolution equation (5), which originally only employed the approximate formula for bubble radii much bigger than the resolution shell. With this approximation, resolution for small bubbles is greatly overestimated. After inserting the exact formula, steady state resolution and with it fission gas release were drastically reduced, and the good agreement of code results /45/ with experimental data /46/ was lost. Therefore, the resolution parameter was enlarged until agreement was reached again. As has been noted already /13/, there is a large uncertainty in this parameter with experimental results reported up to a factor of 40 higher than the theoretical value originally contained in LANGZEIT /44/. In view of this, the necessary enlargement by a factor of 6 seems tolerable. Transient fission gas behaviour is not noticeably influenced by the change.

Fig. 3 shows the LANGZEIT-results after parameter variation compared to experimental gas release data from EBR-II irradiation tests, as fitted by Dutt et al. /47/, and from the Debenelux Fast Breeder Program irradiation tests /46/. Agreement is good, with LANGZEIT staying close to the Debenelux data at lower burn-up, for which there is some disagreement of the experimental results. The figure is similar to one reported earlier /45/. Recently a number of transient tests with irradiated fuel suitable for evaluation with a fission gas behaviour model have been carried out. The first one was the transient gas release test FGR-15 performed at HEDL /48/. Direct electrical heating was used to simulate a slow temperature transient, and time dependent gas release was measured. Fig. 4 shows a comparison of the experimental data with those calculated by LANGZEIT/KURZZEIT. The big initial gas release comes from open porosity and is due to the choice of starting conditions-room temperature and normal pressure-, which may not be adequate. On the whole agreement is satisfactory, with KURZZEIT results being a little low over nearly the whole time span. However, the results are in better agreement with newer results reported recently from HEDL /49/. In fig. 5, release data from these tests are plotted as a function of the mean temperature in the unrestructured zone for thermal ramp rates of 100-200°K /s. Details of the tests are not available at present, but for a first comparison the FGR-15 calculational results were transformed and added to the plot.The slight overestimation of release is probably due to the missing treatment of stress-strain effects.
These direct electrical heating experiments should not be overestimated since due to the heating technique the temperature profile is inverted, though the temperature gradient is typical for LOF conditions.
In-core transient experiments are being performed at Sandia Laboratories and the result of the first series of tests was recently published /10/. The power distribution in the test pins is not typical in this series with a high flux peak at the outer edge. Multiple pulsing is used in the tests to allow the temperature profile to invert in the interval between pulses by losing heat to the cladding. At the end of the transient, the temperature gradient in the unrestructured zone is in the right direction and about representative for LOF situations, but the temperature profile in the inner regions is flat. Moreover, the temperature gradient is

inverted in the first part of the transient. Therefore, one should not attach too much significance to a comparison with this first series, but since LANGZEIT/KURZZEIT is not a fully parametric code, it should be able to yield meaningful answers. During the test, the pin is filmed and transient swelling is deduced from the pictures. In fig.s 6 and 7, the results of two experiments are compared to LANGZEIT/KURZZEIT results for two grain diameters, with 2a=12µm being the more probable value. There is qualitative agreement, but swelling is underestimated by a factor of 2.
A discussion of the reasons for this discrepancy leads directly to some of the deficiencies of the code as it stands now. Already during the presentation of the formalism, part of the unsolved problems have been touched, some of them minor ones that need not be repeated. The more serious ones will be listed here:

a. The most urgent improvement to be done is the inclusion of a stress-strain model and of high temperature creep data. Some preparations have been made already, i.e. inclusion of a hydrostatic pressure in the Van-der-Waals equation (9), and calculation of the whole fuel element cross section at a time to facilitate radial coupling.

b. Transient non-instantaneous gas release from open porosity and transient deformation of porosity must be modeled.

c. Effects of stoichiometry need to be accounted for.

d. Volatile fission products (cesium) should be modeled.

e. As probably a last step in code improvement, parameters should once more be carefully evaluated.

It is planned to make all these improvements without changing the present character of the code, i.e. keeping it fast and simple. Thus it will have to be constantly calibrated with experiments and more refined codes. The comparisons done so far indicate, that this goal can be reached.

Table of symbols

a, a^*	grain radius, grain boundary radius
a_g	acceleration of gravity
a_m	mean distance for bubble release after melting
b, b^*	gas concentration in intra-, intergranular bubbles
b^*_{max}	maximum intergranular gas concentration of gas in bubbles
b_o	gas concentration in 100% open pores
b_i	concentration of gas in bubble group i after melting
B	probability for released intragranular bubble to hit intergranular bubble
B_{max}	maximum fraction of grain boundary covered with bubbles
c, c^*	concentration of resolved intra-, intergranular gas
c_m	concentration of resolved gas after melting
C_1, C_2, C_3	correction factors for coalescence
d	thickness of resolution shell
D_g	diffusion coefficient of resolved gas
D_b, D^*_b	diffusion coefficient of intra-, intergranular bubbles
D_s	surface diffusion coefficient
D_u, D^*_u	uranium self-diffusion coefficient in grain, in grain boundary
F, F^*	function describing release by gas diffusion: intra-, intergranular
F_R, F^*_R	release fraction of intra-, intergranular bubbles

F_i	release fraction in bubble group i after melting
F_p	release fraction from porosity
g, g^*	concentration of gas escaped from grain, from grain boundary
G	number of coalescences
G_{ik}	coalescence rate among bubble groups i,k after melting
k	Boltzmann constant
L	Loschmidt number
L_c	cutoff limit for averaging intergranular bubble parameters
n, n^*	number density of intra-, intergranular bubbles (n^* : per unit surface)
n^*_{vol}	number density of intergranular bubbles per unit volume
n_i	number density of bubbles of group i after melting
n_a, n^*_a	number of atoms per intra-, intergranular bubble
dO	fraction of grain surface in contact with porosity
P	local hydrostatic pressure
p_o, p_1	initial pressure and pressure rise with irradiation time
p_{ex}	excess pressure in bubble
$p; p^*$	intra-, intergranular precipitation
Q	rate of gas released to the boundaries
Q_b	rate of released intragranular gas adding to intergranular bubbles
Q_s	surface diffusion heat of transport
r, r^*	radius of intra-, intergranular bubbles

r_{eq}, r^*_{eq}	equilibrium radius of intra-, intergranular bubbles
r_i	bubble radius for group i after melting
r^*_{max}	maximum radius of intergranular bubbles
r^*_{eff}	radius of spherical bubble with same volume as lenticular bubble
r_z, r^*_z	cell radius for intra-, intergranular bubbles
R, R^*	intra-, intergranular resolution
R_g	universal gas constant
s, s^*	distance traveled by intra-, intergranular bubble during the transient
s_i	distance traveled by bubble of group i after melting
S_b	rate of intergranular gas released by bubble migration
S, S^*	intra-, intergranular swelling
S_n	swelling after melting
t	time of irradiation or transient or melting
T	temperature
∇T	bulk thermal gradient
∇T_s	thermal gradient at bubble surface
v, v^*	velocity of intra-, intergranular bubbles
w	Van-der-Waals constant
X	planar cell width for vacancy diffusion from grain to grain boundary

x_i	zeros of zeroth order Bessel-function
δz	grain boundary width
α	volume factor of lenticular bubbles
β	rate of gas formation by fission
γ	surface tension of fuel
η	resolution parameter
κ	kinematic viscosity of molten fuel
μ	viscosity of molten fuel
ν	surface density of uranium atoms
ψ	contact angle of intergranular bubbles
ρ	density of fuel
τ	reduced time for calculation of transient release by gas diffusion
Ω	molecular volume

Literature

/1/ L.W. Deitrich, J.F. Jackson:
"The Role of Fission Product in Whole Core Accidents";
IAEA Specialists Meeting on Role of Fission Products in Whole Core Accidents, Harwell. UK, June 1977 (IWGFR/19)

/2/ L.W. Deitrich:
"An Overview of Fission Gas Effects in Hypothetical Fast Reactor Accidents";
Transact. Am. Nucl. Soc. 28, 231, 1978

/3/ A.R. Baker, H.J. Teagne:
"The Role of Fission Products in Whole Core Accidents";
IAEA Specialists Meeting on Role of Fission Products in Whole Core Accidents, Harwell, June 1977 (IWGFR/19)

/4/ R.B. Poeppel:
"An Advanced Gas Release and Swelling Subroutine";
Proc. Conf. on Fast Reactor Fuel Element Technology, New Orleans, 1971

/5/ E.E. Gruber, L.W. Deitrich:
"Dispersive Potential of Irradiated Breeder Reactor Fuel During a Thermal Transient";
Transact. Am. Nucl. Soc. 27, 577, 1977

/6/ R.G.Esteves , A.R. Wazzan, D. Okrent:
"Simulation of Non-Equilibrium Fission Gas Behaviour During Fast Thermal Transients";
Nucl. Eng. and Design 45, 343, 1978

/7/ J.R. Hofmann, C.C.Meck:
"Internal Pressurization in Solid Mixed-Oxide Fuel Due to Transient Fission Gas Release";
Nucl. Sci. Eng. 64, 713, 1977

/8/ M.H. Wood:
"A Model to Describe the Role of Non-Equilibrium Intragranular Fission Gas Bubbles During Transient Heating";
Journ. Nucl. Mat. 78, 58, 1978

/9/ R.W. Ostensen:
"FISGAS - A Code for Fission-Gas Migration and Fuel Swelling in a LMFBR Accident";
SAND-78-1790 to be released, Sandia Laboratories, Albuquerque N.M.

/10/ G.L. Cano, R.W. Ostensen, M.F. Young:
"Visual in-Pile Fuel Disruption Experiments";
to be published in Nucl. Technology.

/11/ E.H. Randklev, C.A. Hinmann:
"Fission Gas Behaviour in Mixed-Oxide-Fuel During Overpower and Thermal Transient Tests";
Intern. Conf. on Fast Breeder Reactor Fuel Performance, Monterey, Calif. 5.-8.3.1979

/12/ H.G. Bogensberger, C. Ronchi:
"Effects Due to Fission Gas During Unprotected Overpower Transients in a Liquid-Metal Fast Breeder Reactor";
Nucl. Techn. 29, 73, 1976

/13/ E.A. Fischer:
"Analysis of Experimental Fission Gas Behaviour Data in Fast Reactor Fuel under Steady State and Transient Conditions";
KfK 2370, 1977

/14/ E.A. Fischer, L. Väth:
"The Karlsruhe Approach to Modeling Fission Gas Behaviour for Fast Reactor Accident Analysis";
Transact. Am. Nucl. Soc. 31, 367, 1978

/15/ E.E. Gruber:
"A Generalized Parametric Model for Transient Gas Release and Swelling in Oxide Fuels";
Nucl. Techn. 35, 617, 1977

/16/ J.A. Turnbull:
"The Distribution of Intergranular Fission Gas Bubbles in UO_2 During Irradiation";
Journ. Nucl. Mat. 38, 203, 1971

/17/ C. Ronchi:
"Physical Processes and Mechanisms Related to Fission Gas Swelling in MX-Type Nuclear Fuels";
Journ. Nucl. Mat. 84, 55, 1979

/18/ F.S. Ham:
"Theory of Diffusion-Limited Precipitation";
Journ. Phys. Chem. Solid 6, 335, 1958

/19/ R.S. Nelson:
"The Stability of Gas Bubbles in an Irradiation Environment";
Journ. Nucl. Mat. 31. 153. 1969

/20/ C. Ronchi, Hj. Matzke:
"Calculations on the In-Pile Behaviour of Fission Gas in Oxide Fuels";
Journ. Nucl. Mat. 45, 15, 1972/73

/21/ J.M. Griesmeyer , N.M. Ghoniem:
"A Dynamic Intragranular Fission Gas Behaviour Model";
NUREG/CR-0906, 1979

/22/ W. Chubb, W. Storhok, D.L. Keller:
"Observations Relating to the Mechanisms of Swelling and Gas Release in Uranium Dioxide at High Temperatures";
Journ. Nucl. Mat. 44, 136, 1972

/23/ B.J. Buescher, R.O. Meyer:
"Thermal Gradient Migration of Helium Bubbles in Uranium Dioxide";
Journ. Nucl. Mat. 48, 143, 1973

/24/ E.E. Gruber:
"Calculated Size Distributions for Gas Bubble Migration and Coalescence in Solid";
Journ. Appl. Phys. 38, 243, 1967

/25/ F.A. Nichols:
"Kinetics of Diffusional Motion of Pores in Solids";
Journ. Nucl. Mat. 30, 143, 1969

/26/ G.W. Greenwood, A.E.J. Foreman, D.E. Rimmer:
"The Role of Vacancies and Dislocations in the Nucleation and Growth of Gas Bubbles in Irradiated Fissile Material".
Journ. Nucl. Mat. 4, 305, 1959

/27/ M.H. Wood, M.R. Hayns:
"A Current View of the Theory of Fission Gas Precipitation into Intra- and Intergranular Porosity";
Proceedings of the Workshop on Fission Gas Behaviour in Nuclear Fuels, Karlsruhe, October 26.-27., 1978
(EUR-6600 EN)

/28/ J.R. Matthews, M.H. Wood:
"Modelling the transient behaviour of fission gas";
Journ. Nucl. Mat. 84, 125, 1979

/29/ A.J. Markworth:
"Growth Kinetics of Inert-Gas Bubbles in Polycrystalline Solids";
Journ. Appl. Phys. 43, 2047, 1972

/30/ A.J. Markworth:
"On the binding between gas bubbles and grain boundaries";
Mat. Sci. Eng. 6, 391, 1970

/31/ M.O. Tucker:
"The spacing of intergranular fission gas bubbles in irradiated UO_2";
Journ. Nucl. Mat. 74, 34, 1978

/32/ M.O. Tucker:
"The transfer of fission gas between grain faces and edges in UO_2";
Journ. Nucl. Mat. 75, 282, 1978

/33/ M.O Tucker:
"Relative growth rates of fission-gas bubbles on grain faces";
Journ. Nucl. Mat. 78, 17, 1978

/34/ E.E. Gruber:
"Migration and coalescence of fission gas bubbles in oxide fuels by surface diffusion";
Proc. Int. Conf. "Physical metallurgy of reactor fuel elements",
Berkeley, England, 2.-7.8.1973, p. 238

/35/ D. Hull, D.E. Rimmer:
"The Growth of Grain-Boundary Voids Under Stress";
Philos. Mag. 4, 673, 1959

/36/ R.J. Di Melfi, L.W. Deitrich:
"The effect of grain boundary gas on transient fuel behaviour";
Nucl. Technol. 43. 328 (1979)

/37/ K. Maschke et al:
"A note on Percolation Probabilities";
Phys. Stat. Sol. (b) 60, 563 (1973)

/38/ M. Dalle Donne, M.P. Ferranti :
"The growth of vapor bubbles in superheated sodium";
Int. Journ. of Heat and Mass Transfer, 18, 477 (1975)

/39/ R.S. Brodkey:
"The phenomena of fluid motions";
Reading-Mass., Addison-Wesley 1967, p. 109

/40/ M.R. Hayns, M.H. Wood:
"On the rate theory model for fission-gas behaviour in nuclear fuels";
Journ. Nucl. Mat. 59, 293 (1976)

/41/ B. Burton, G.L. Reynolds:
"The sintering of grain boundary cavities in uranium dioxide";
Journ. Nucl. Mat. 45, 10 (1972/73)

/42/ W. Beeré, G.L. Reynolds:
"The morphology and growth rate of interlinked porosity in irradiated UO_2";
Journ. Nucl. Mat. 47, 51 (1973)

/43/ H.C. Tsai, D.R. Olander:
"The Viscosity of Molten Uranium Dioxide";
Transact. Am. Nucl. Soc. 15, 211 (1972)

/44/ J.A. Turnbull, R.M. Cornell:
"The resolution of fission-gas atoms from bubbles during the irradiation of UO_2 at an elevated temperature";
Journ. Nucl. Mat. 41, 156 (1971)

/45/ E.A. Fischer:
"The Role of Fission Gas in the Analysis of Hypothetical Core Disruptive Accidents";
IAEA Specialists Meeting on Role of Fission Products in Whole Core Accidents, Harwell, June 1977 (IWGFR/19)

/46/ H. Zimmermann:
"Spaltgasverhalten in Oxid-Brennelementen für Schnelle Brüter";
KfK 2057 (1974)

/47/ D.S. Dutt et al:
"A Correlated Fission Gas Release Model for Fast Reactor Fuels";
Transact. Am. Nucl. Soc. 15, 198 (1972)

/48/ E.T. Weber et al:
"Laboratory Studies on Melting and Gas Release Behaviour of Irradiated Fuel";
Conf. on Fast Reactor Safety, Beverly Hills, Calif. April 1977

/49/ E.H. Randklev, C.A. Hinmann:
"Fission gas behaviour in mixed-oxide fuel during over-power and thermal transient tests";
Intern. Conf. on Fast Breeder Reactor Fuel Performance, Monterey, Calif. 5.-8.3.1979

/50/ J.A. Turnbull, C.A. Friskney:
"The release of fission products from nuclear fuel during irradiation by both lattice and grain boundary diffusion";
Journ. Nucl. Mat. 58, 31 (1975)

Acknowledgement

My thanks go to Mr. E. Fischer for helpful discussions and for reviewing the manuscript, and to Mrs. Lepoittevin for typing the script.

Temperature /°K/	$D_{lattice}$ /cm^2/sec/	$D_{grain\ boundary}$ /cm^2/sec/
1600	1.6 - 15	1.0 - 9
2000	1.7 - 12	7.9 - 8
2400	1.7 - 10	1.5 - 6
2800	4.7 - 9	1.2 - 5

$r^* \approx$ 5.-5 $\qquad\qquad$ $\delta_z \approx$ 1.-8

Table 1: Diffusion coefficient for uranium self diffusion in the lattice and on the grain boundary and characteristic dimensions

Table 2 : Parameters for LANGZEIT/KURZZEIT

Symbol	Meaning	Value	Literature
B_{Max}	maximum grain surface fraction covered by intergranular bubbles	.5	/40/
d	thickness of resolution shell	10^{-9} m	/13/
D_g	diffusion coefficient of resolved gas (T in ^oK, ß in mole $m^{-3}s^{-1}$)	$2.5 \cdot 10^{-5} \exp(-4.8 \cdot 10^4/T) + 4.5 \cdot 10^{-15}$ ß $/m^2/s/$	/12/
D_s	surface diffusion coefficient	$57 \cdot \exp(-5.44 \cdot 10^4/T)$ $/m^2/s/$	/13/
D_u	uranium self diffusion coefficient in grain	$2 \cdot 10^{-4} \exp(-5.56 \cdot 10^4/T)$ $/m^2/s/$	/8/
D_u^*	uranium self diffusion coefficient in boundary	$3 \cdot 10^{-4} \exp(-3.49 \cdot 10^4/T)$ $/m^2/s/$	/41/
n_o	initial intragranular bubble number density	10^{21} $/m^{-3}/$	/13/
h_o^*	initial intergranular bubble number density	10^{12} $/m^{-2}/$	/29, 40/
L_c	cutoff limit for averaging intergranular bubble parameters	.2	

Table 2 continued

Symbol	Meaning	Value	Literature
$\bar{d}O$	fraction of grain surface in contact with porosity	.1	
Q_s	surface diffusion heat of transport	6.95 J	/13, 15, 28/
W	Van-der-Waals constant	$4.926 \cdot 10^{-5}$ m^3/mole	/13/
δz	width of grain boundaries	$5 \cdot 10^{-10}$ m	/42/
Y	fission yield of noble gases	27.5%	/13/
γ	surface tension of uranium dioxide	.8 J/m^2 if $T \leq 1700$ .56J/m^2 if $T \geq 1900$ linear interpolation in between	/13/
κ	kinematic viscosity of molten fuel	10^{-6} m^2/s	/43/
Ψ	contact angle of intergranular bubbles	50^o	/42/
η	resolution parameter	9.3ß (s^{-1})	
Ω	atomic volume	$4.08 \cdot 10^{-29}$ m^3	/4,6,21,28/

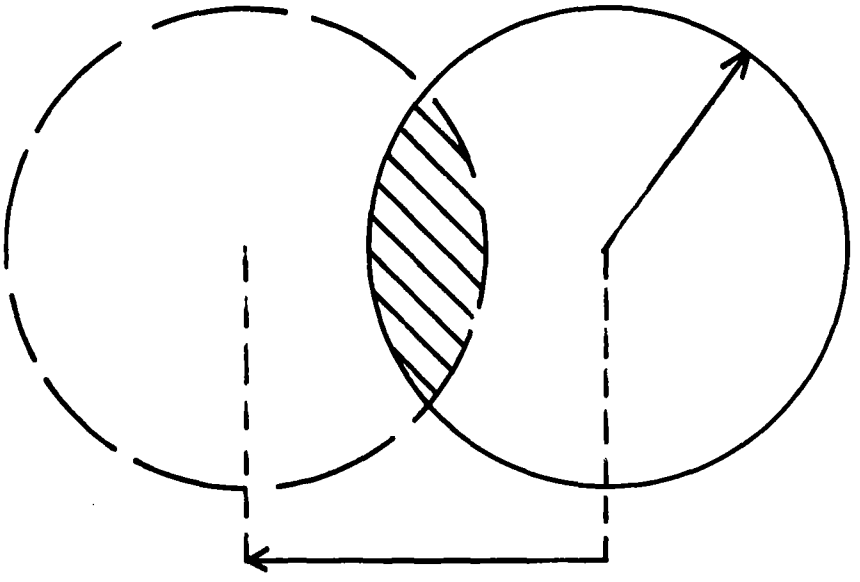

Fig. 1: Illustration of gas release by bubble migration. Right circle: Grain; left circle: Virtual position of bubbles after traveling distance s; shaded area: Region of unreleased bubbles.

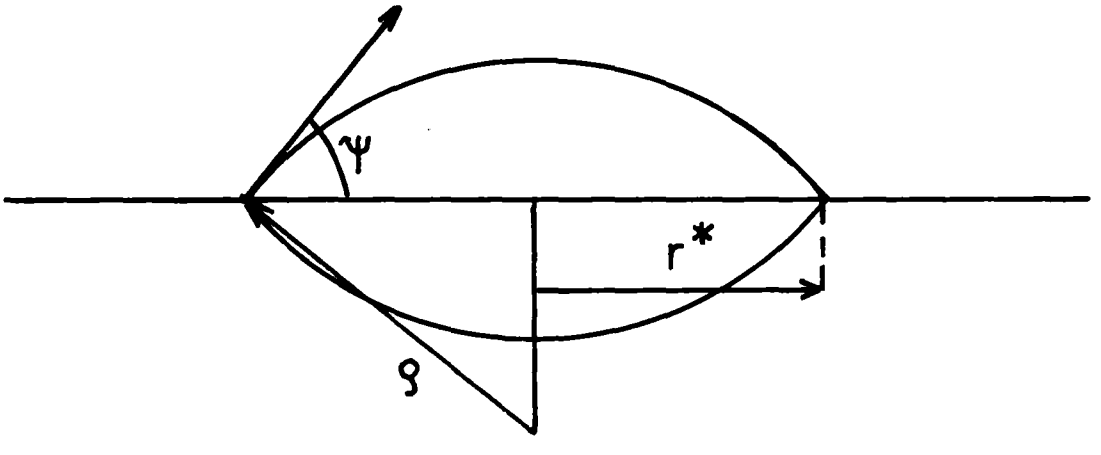

Fig. 2: Shape of intergranular bubble.
ϱ: Radius of curvature.

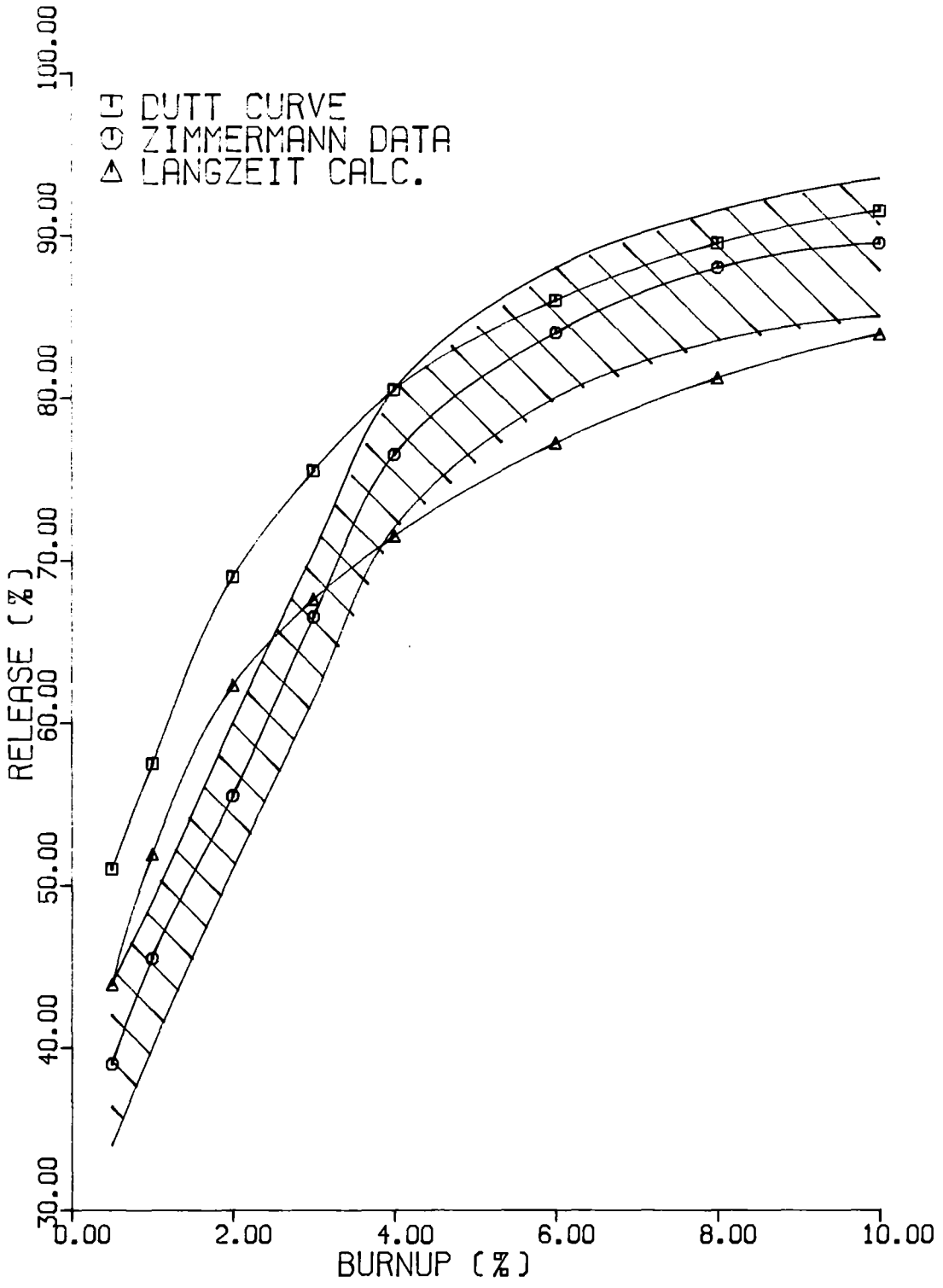

FIG. 3 COMPARISON WITH IRRADIATION DATA

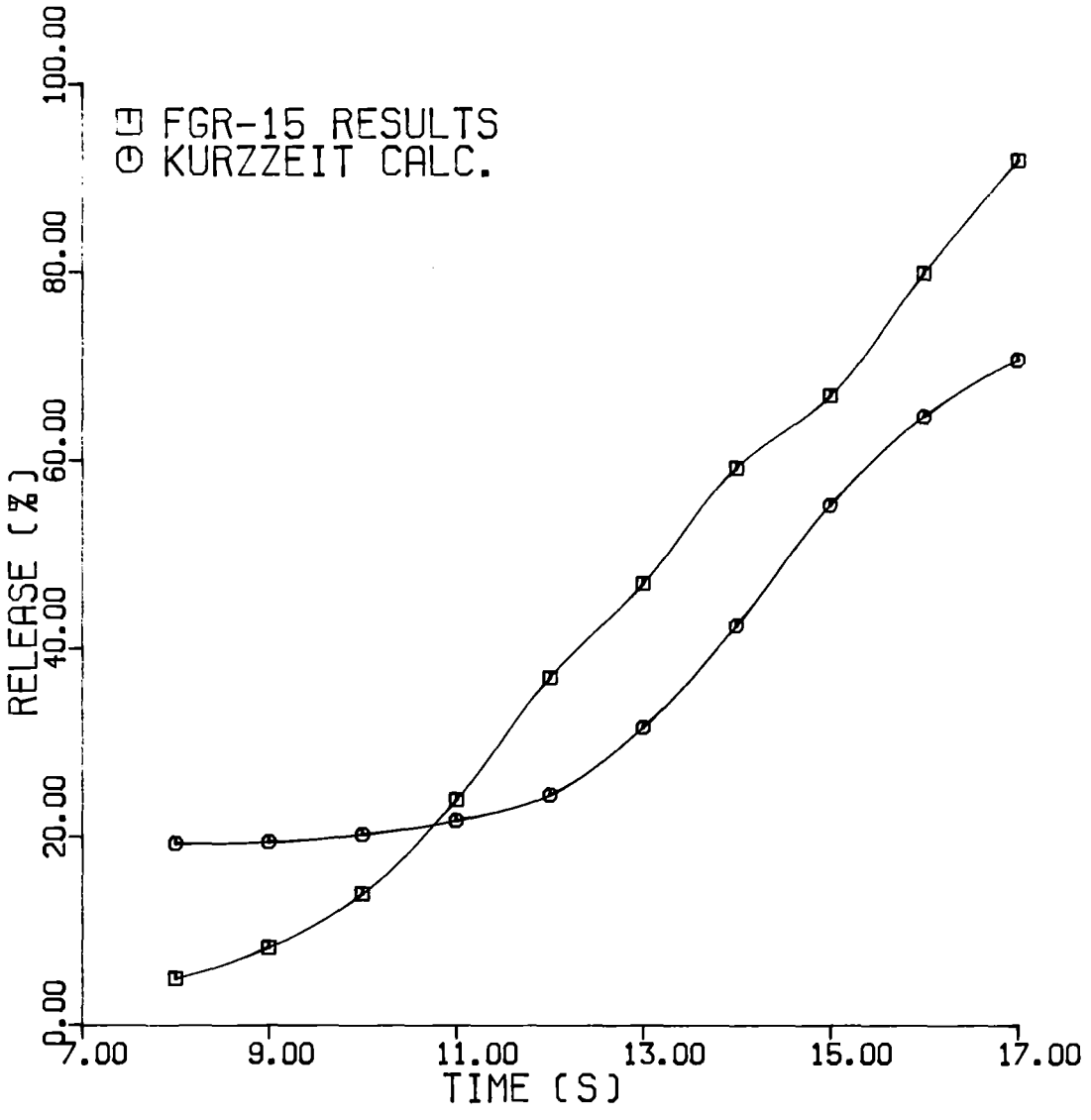

FIG. 4 HEDL DEH-EXPERIMENT FGR-15

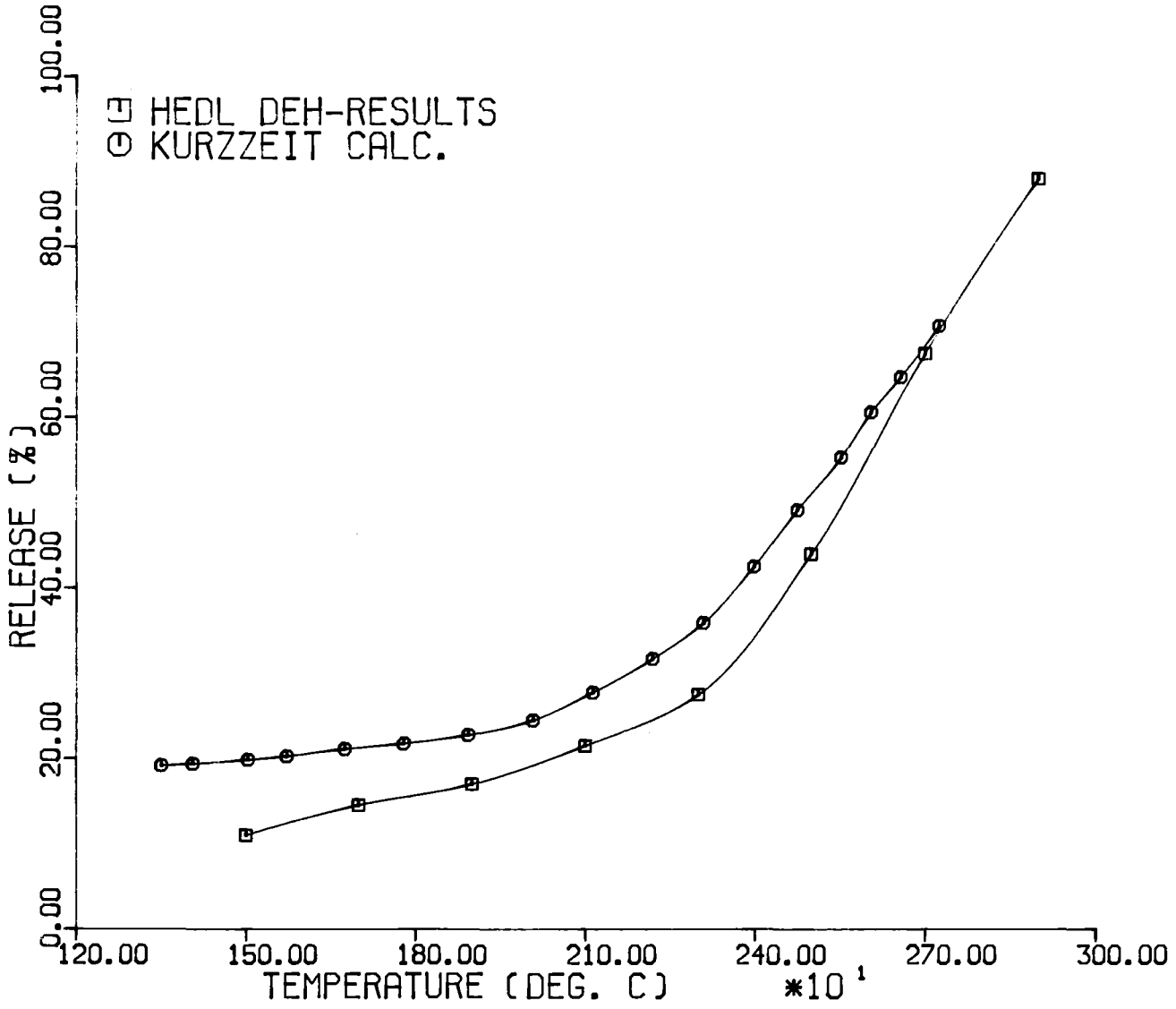

FIG. 5 SUMMARY OF HEDL DEH-EXPERIMENTS

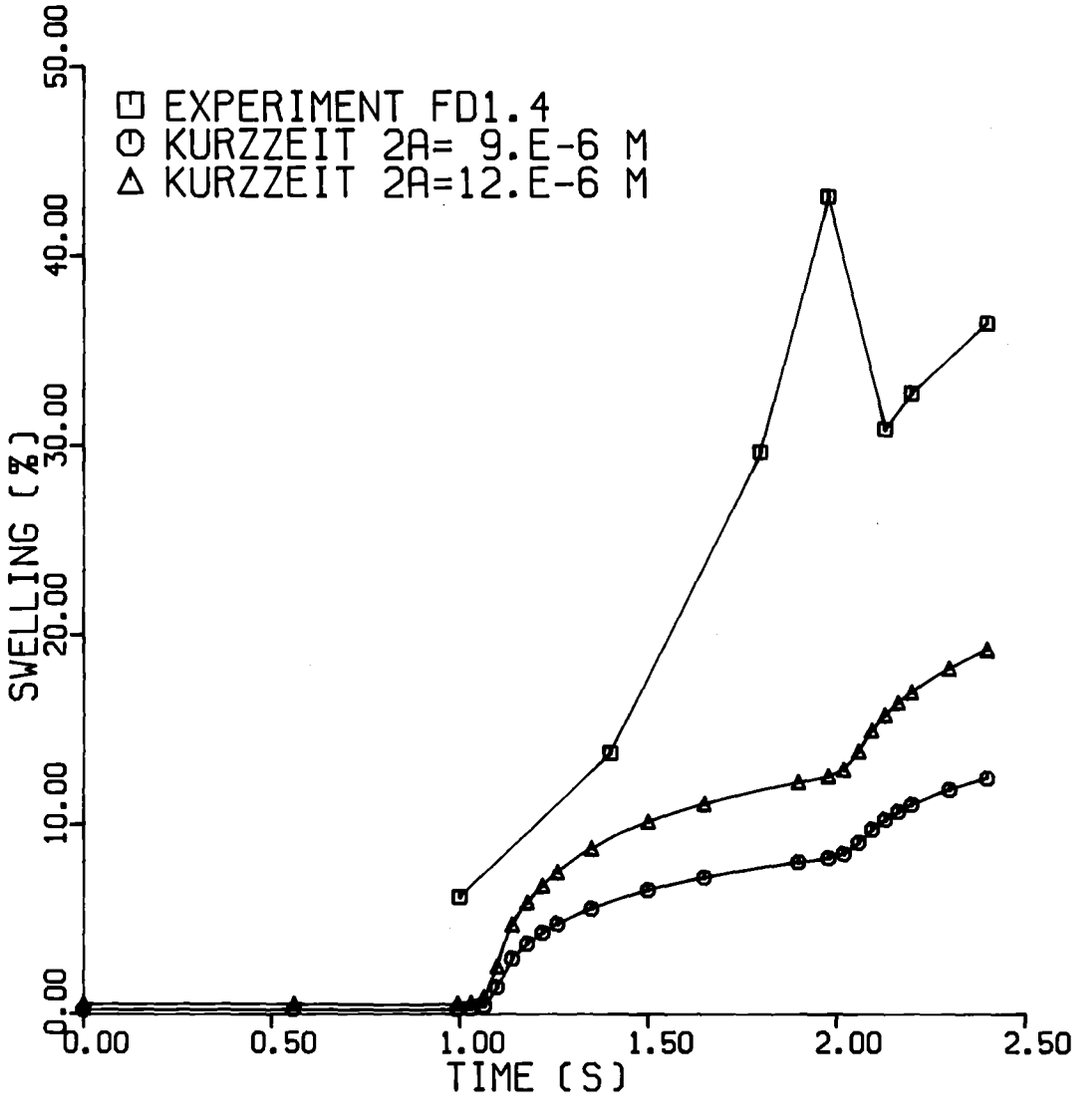

FIG. 6 SANDIA IN-PILE EXPERIMENT FD1.4

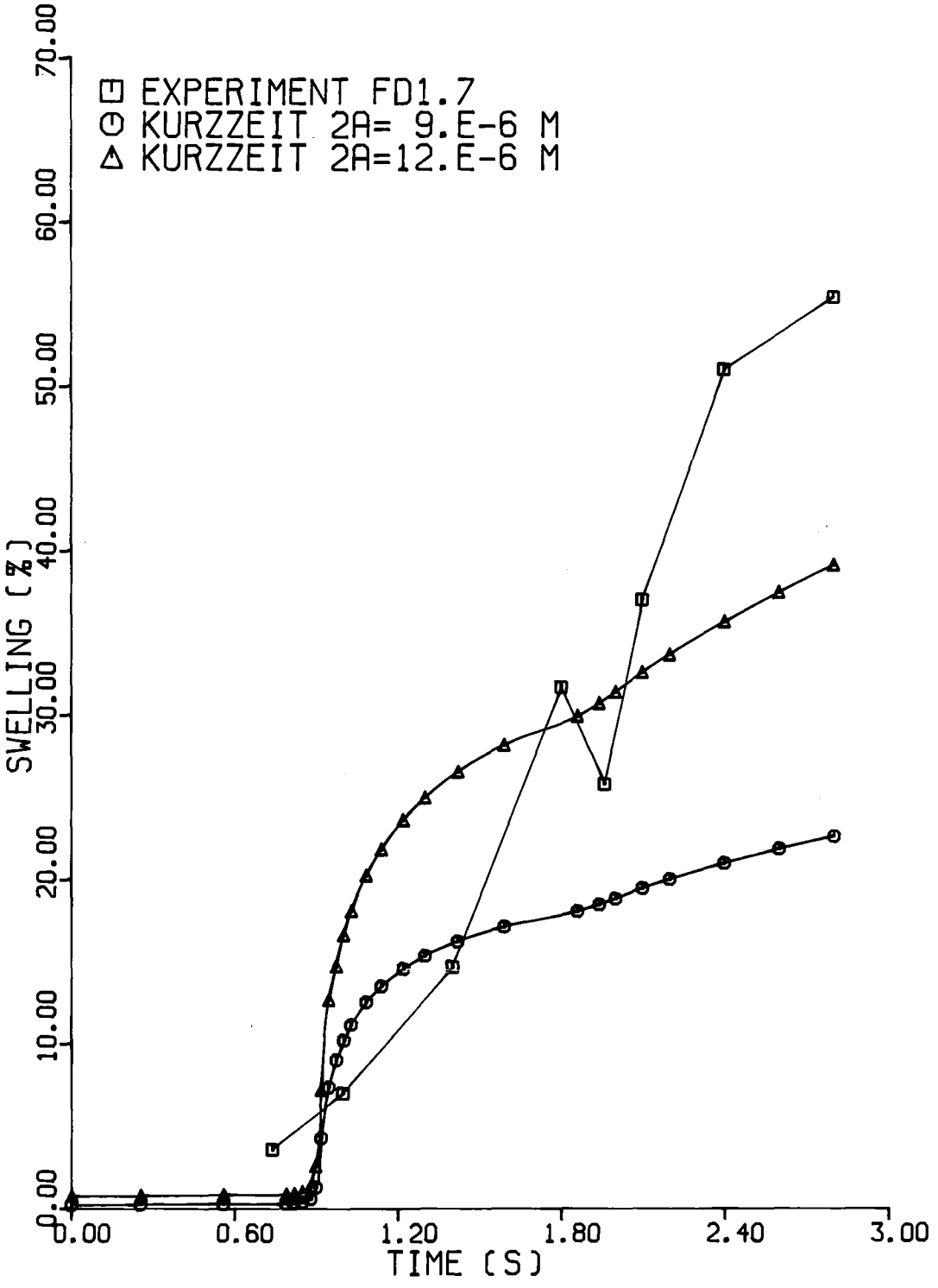

FIG. 7 SANDIA IN-PILE EXPERIMENT FD1.7